Mechanistic basis for low threshold mechanosensitivity in voltage-dependent K^+ channels

Daniel Schmidt[1], Josefina del Mármol, and Roderick MacKinnon[2]

Howard Hughes Medical Institute, Laboratory of Molecular Neurobiology and Biophysics, Rockefeller University, 1230 York Avenue, New York, NY 10065

Edited by Christopher Miller, HHMI, Brandeis University, Waltham, MA, and approved May 2, 2012 (received for review March 20, 2012)

Living cells respond to mechanical forces applied to their outer membrane through processes referred to as "mechanosensation". Faced with hypotonic shock, to circumvent cell lysis, bacteria open large solute-passing channels to reduce the osmotic pressure gradient. In the vascular beds of vertebrate animals blood flow is regulated directly through mechanical distention-induced opening of stretch-activated channels in smooth muscle cells. Touch sensation is thought to originate in mechanically sensitive ion channels in nerve endings, and hearing in mechanically sensitive ion channels located in specialized cells of the ear. While the ubiquity of mechanosensation in living cells is evident, the ion channels underlying the transduction events in vertebrate animals have remained elusive. Here we demonstrate through electrophysiological recordings that voltage-dependent K^+ (Kv) channels exhibit exquisite sensitivity to small (physiologically relevant in magnitude) mechanical perturbations of the cell membrane. The demonstrated mechanosensitivity is quantitatively consistent with membrane tension acting on a late-opening transition through stabilization of a dilated pore. This effect causes a shift in the voltage range over which Kv channels open as well as an increase in the maximum open probability. This mechanically induced shift could allow Kv channels and perhaps other voltage-dependent ion channels to play a role in mechanosensation.

electrophysiology | potassium channel | gigaseal | gating | membrane forces

The only form of mechanosensation for which we have a good molecular understanding is that mediated by mechanosensitive channels in bacteria (1, 2). The mechanosensitive channel of large conductance (MscL) is a membrane-stretch-activated channel that opens when bacteria swell under hypotonic conditions, as occurs when it rains. Under high membrane tension MscL channels open wide enough to allow molecules up to a size of about 40 kDa to pass through their pore, relieving an osmotic pressure gradient that would otherwise lead to cell lysis and death. Tension gating of MscL channels was demonstrated and characterized through isolation of channels in gigaseal patches and recording electrical current as a function of membrane tension induced while applying pressure to the pipette (3, 4). A molecular mechanism of channel opening in response to tension has been proposed on the basis of atomic structures, electron paramagnetic resonance (EPR) spectroscopic studies and molecular modeling (5–8).

Stretch activation of ion channels from eukaryotic cells, including Kv channels, has been studied using the same method of pipette pressurization (9, 10). Pressurization of a gigaseal patch has been shown in a number of cases to alter channel gating, however, the method has an important limitation. A gigaseal membrane patch is already under considerable baseline tension prior to the application of pressure. The baseline tension of the membrane in a gigaseal patch originates in the adherence of lipid to glass, which is the basis of an electrical gigaseal, and in magnitude is in the range of 0.5 to 4 mN/m (11). This tension range is quite high when one considers that membrane lysis occurs in the range 10–20 mN/m. The study of stretch activation using gigaseal patches therefore is appropriate for high threshold mechanosensitive channels such as MscL, which have evolved to open only under near lytic tensions (i.e., higher than the baseline tension of the gigaseal patch), but may not be appropriate for channels that may exhibit a lower tension threshold because tension induced changes may have already occurred through the act of gigaseal formation, prior to pressurization. Many forms of mechanosensation in eukaryotic cells, we suspect, will result from alterations of gating that occur with small mechanical perturbations of the membrane as a result of such low threshold sensitivity to membrane tension.

In an earlier study of Kv channels we observed large gating differences between whole cell and gigaseal configurations. After excluding various mechanisms such as gating modulation due to cytoplasmic regulatory factors, we attributed these differences to the increased membrane tension intrinsic to the gigaseal patch. In the present study we examine this effect further by addressing the following questions: (*i*) Are similar gating changes induced in different K^+ channels? If membrane tension is acting on a fundamental gating transition such as channel opening, then we should expect the effect to occur in other Kv channels; (*ii*) Is it possible to replicate similar gating changes in Kv channels by applying tension to the cell membrane in a manner other than gigaseal formation, such as osmotic swelling of whole cells? (*iii*) What value of tension is required to produce a physiologically relevant change in channel open probability? In other words, how low is the mechanical threshold for Kv channel activation? To address this question we develop a theory to explain the effects of membrane tension on gating and, within the context of this theory, estimate the functional relationship between membrane tension and channel open probability.

Results

The Effect of Gigaseal Formation on Kv Channel Gating. The formation of gigaseal membrane patches on *Xenopus* oocytes induces an alteration or "conversion" of gating properties in Kv channels, as depicted for the mutant of Kv1.2 called the Kv1.2 paddle chimera channel (12) (Fig. 1 *A–D*). When a gigaseal patch is first formed the gating properties are similar to those recorded in whole-cell mode using two-electrode voltage clamp (Fig. 1 *A* and *D* black). Then, over time, changes occur that include (*i*) a shift in the voltage-activation curve to more negative membrane voltages, (*ii*) a steepening of the activation curve, and (*iii*) an increased maximum current when the activation curve saturates, which reflects an increased open probability, not an increased channel number or single channel conductance (13) (Fig. 1 *B–D*, blue and red). This conversion occurs independent of patch configuration and even when the inside of the patch is kept in direct communica-

Author contributions: D.S., J.d.M., and R.M. designed research; D.S. and J.d.M. performed research; D.S., J.d.M., and R.M. analyzed data; and D.S., J.d.M., and R.M. wrote the paper.

The authors declare no conflict of interest.

This article is a PNAS Direct Submission.

[1]Present address: MIT Media Lab, 20 Ames Street, Cambridge, MA 02139.

[2]To whom correspondence should be addressed. E-mail: mackinn@rockefeller.edu.

This article contains supporting information online at www.pnas.org/lookup/suppl/doi:10.1073/pnas.1204700109/-/DCSupplemental.

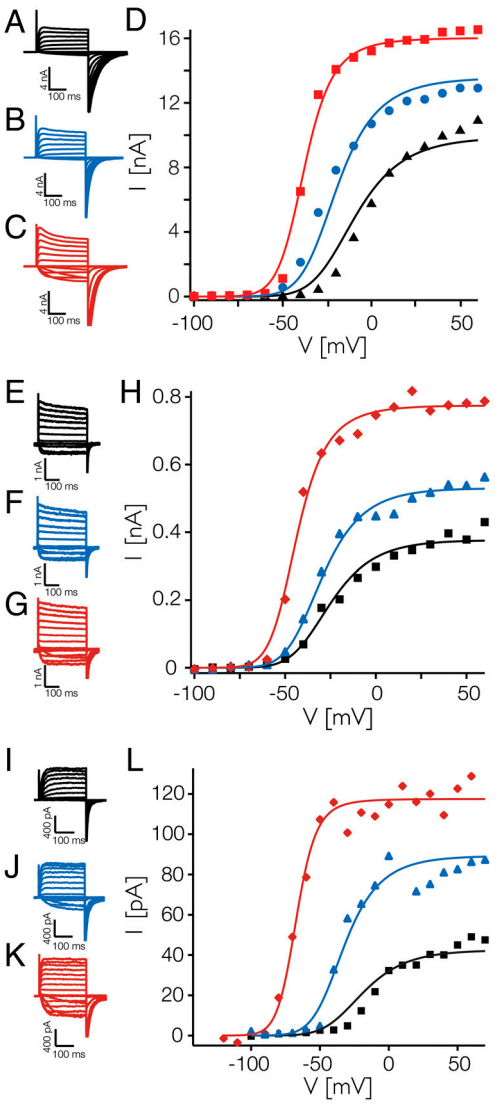

Fig. 1. *The Effect of Membrane Forces.* (*A–D*), Paddle Chimera in the same outside-out patch with 0 mmHg (*A*, black), 5 mmHg (*B*, blue) and 15 mmHg (*C*, red) of transient pressure applied. Voltage pulses *A–C*: h.p. −100 mV to 60 mV, $\Delta V = 10$ mV. *D*, The solid curves are fit globally to the data from (*A–C*) with Eq. **1** (see main text) using the relationship $\langle I \rangle = iNP_O$: L(0 mmHg) = 1.5± 0.15, L(5 mmHg) = 4.7 ± 0.71, L(15 mmHg) = 39.9 ± 11.6, $V_m = -29 \pm 2$ mV, $z = 1.25 \pm 0.09$ q_e, iN = 16423 ± 340. (*E–H*), Shaker Kv in the same outside-out patch at different time points after patch excision: 0 min (*E*, black), 4 min (*F*, blue) and 8 min (*G*, red). Voltage pulses *E–G*: h.p. −100 mV to 60 mV, $\Delta V = 10$ mV. h, The solid curves are fit globally to data from (*E–G*) with Equation **1** (see text) using the relationship $\langle I \rangle = iNP_O$: L(t = 0 minutes) = 1.8 ± 0.11, L(t = 4 minutes) = 4.5 ± 0.41, L(t = 8 minutes) = 62.2 ± 15, $V_m = -41.5 \pm 1$ mV, $z = 1.75 \pm 0.09$ q_e, iN = 1017 ± 12. (*I–L*) Kv2.1 channels in the same on-cell patch with 0 mmHg (*I*, black), 5 mmHg (*J*, blue) and 15 mmHg (*K*, red) of transient pressure applied. Voltage pulses *I–J*: h.p. −100 mV to 70 mV, $\Delta V = 10$ mV, K: h.p. −120 mV to 60 mV, $\Delta V = 10$ mV. L, The solid curves are fit globally to data from (*I–K*) with Eq. **1** (see main text) using the relationship $\langle I \rangle = iNP_O$: L(0 mmHg) = 0.56 ± 0.05, L(5 mmHg) = 3.1 ± 0.41, L(15 mmHg) = 165 ± 86.1, $V_m = -46.8 \pm 2.7$ mV, $z = 1.2 \pm 0.1$ q_e, iN = 118 ± 2.2.

tion with the cytoplasm (i.e., on-cell configuration or an inside-out patch reinserted into the oocyte). The rate of conversion is variable, but transient application of pressure to the pipette speeds the process. Conversion is irreversible and once complete no further changes are observed. The final gating properties of channels within a patch of membrane inside the pipette after conversion are similar, independent of patch configuration (on-cell, inside-out or outside-out).

We tested whether gigaseal formation affects gating in two other Kv channels: Shaker (Kv1.1 from drosophila) and Kv2.1 (Fig. 1 *E–L*). As in the Kv1.2 paddle chimera channel, gigaseal formation caused the voltage-activation curves to shift to more negative voltages, to become steeper, and to reach a larger maximum current value. The qualitatively similar effect on all three channels suggests that gigaseal formation influences an aspect of gating that is common to all three channels.

Fig. 2 shows a variation on the experiments described in Fig. 1. Here Kv1.2 paddle chimera channels expressed in Sf-9 cells are recorded first in on-cell configuration after the conversion has occurred (Fig. 2 *A* and *C*). On-cell configuration records currents from channels located on the patch of membrane inside the pipette, as depicted (Fig. 2*D*). Note that these channels exhibit gating properties similar to channels in patches on Xenopus oocytes after conversion. Next, the patch is broken to produce the whole-cell configuration, which records currents from channels located in the cell membrane, not within the pipette (Fig. 2 *B*, *C*, and *E*). The amplitudes cannot be compared (and are thus normalized to unity in Fig. 2*C*) because the two configurations, on-cell and whole-cell, have a different number of channels, however, from the shift and steepening of the activation curve it is evident that channels in the cell membrane are not converted. Thus, only channels within the patch of membrane attached to the pipette undergo conversion, even though channels in the patch maintain the same exposure to the cytoplasm as channels in the cell membrane. The patch of membrane within the pipette is under lateral tension due to the adhesion of lipid to glass on the perimeter surrounding the patch, while the cell membrane is not under tension (Fig. 2 *D* and *E*).

The experiments in Figs. 1 and 2 were carried out using oocytes and Sf-9 cells. We find similar results in mammalian cells as well (Fig. S1). Thus, the effects of lateral membrane tension on channel gating appear to be independent of cell type.

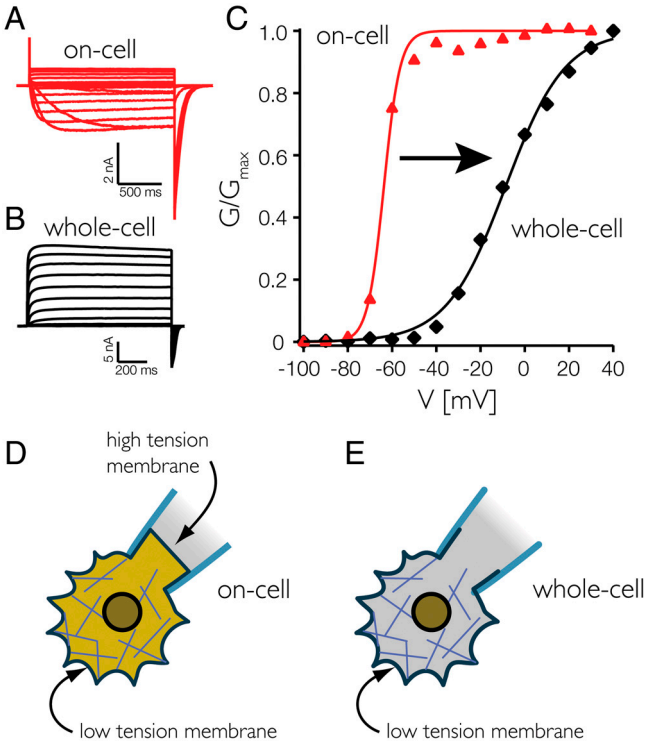

Fig. 2. *The Effect of Membrane Configuration.* Paddle Chimera in on-cell patch (*A*) or whole-cell configuration (*B*) recorded from the same Sf-9 cell. *C*, Boltzmann functions (solid lines) fit data from (*A*) with V_m (mV) and z (q_e): −63.69 ± 0.53, 6.8 ± 0.7 (on-cell patch), and from (*B*) −8.69 ± 0.65, 1.9 ± 0.1 (whole cell).

Demonstration of Lipid Adherence to Polished Glass. The quantitative demonstration that gigaseal patches are under lateral tension involved measurements of patch membrane curvature as a function of pressure applied across the patch (11). The Laplace-Young formula $\gamma = 0.5 * \Delta P * R$, which relates membrane tension γ to pressure difference across the patch ΔP and radius of membrane curvature R, leaves tension undefined at the singularity $\Delta P = 0$, $R = \infty$. Through a simple geometric relation Opsahl and Webb decomposed γ into orthogonal components, which enabled estimation of a constant lateral component of tension that is due to the adhesion of lipid to the polished glass pipette. This component must persist even under zero pressure and by necessity produces membrane tension at zero pressure.

In Fig. 3 we demonstrate qualitatively the effect of polished glass on the tension of a lipid membrane in a different way. A giant unilamellar vesicle (GUV) containing fluorescently labeled lipids can be seen to undergo undulations in which at any instant in time its structure may deviate from a spherical shape, indicating that its membrane is near zero tension (Fig. 3*A*). When a freshly polished glass pipette is brought into contact with the vesicle the vesicle suddenly forms a near perfect sphere, indicating that its tension has increased, and lipids can be seen running along the surface of the glass due to the intrinsic adhesiveness of lipids to a polished glass surface (Fig. 3*B*). Importantly, no suction has been applied to the pipette; the movement of lipids is due to the adhesive force between lipid and polished glass, and the same effect is observed in a polished glass wand without a lumen. The entire experiment is shown in a movie (Movie S1). In this experiment water is squeezed out of the high-tension vesicle, causing it to shrink as lipid flows up the surface of the polished glass pipette. The conclusion we draw from this experiment is that lipids adhere strongly to glass and this adherence creates increased tension in the membrane.

We note that the GUV in this experiment behaves differently than the entire cell in Fig. 2. The entire GUV comes under tension when in contact with polished glass. In contrast, the entire membrane of a cell, because of its folded geometry and cytoskeletal attachments, does not come under tension when placed in contact with polished glass. Only the patch within the pipette comes under tension. In fact, membrane folds and cytoskeletal attachments can explain why even for the patch within the pipette the conversion is not instantaneous, and why application of transient pressure to the pipette, by forcing the lipid into contact with glass, speeds the process of conversion.

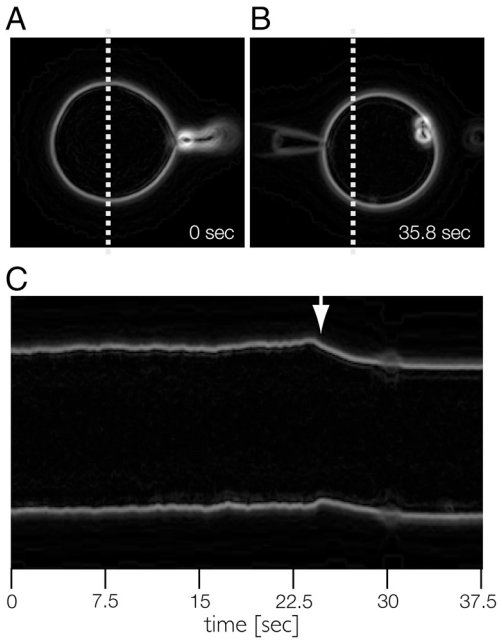

Fig. 3. *Lipid Adheres to Glass. A*, Giant Unilamellar Vesicles (GUVs) formed with DOPC and Rhodamine-DOPE display rapid surface undulations when suspended in aqueous solution. *B*, When brought in contact with a fused borosilicate glass wand the surface undulations of the GUV cease, and lipids slowly run up the wand (left side of GUV). *C*, Kymograph of pixel intensities along the red line indicated in *A* and *B*. The white arrow indicates the time point when the wand touches the GUV.

In a gigaseal patch lipid should flow onto the glass, but only until the energetic cost of removing a lipid molecule from the membrane is balanced by the energy gained when a lipid molecule adheres to the glass pipette. Because the energy cost of removing a lipid molecule from the membrane increases in direct proportion to the membrane tension, an equilibrium tension will be reached when the energetic gains and losses are balanced. This description explains why the conversion goes to completion and then stops, and why the converted channels within a patch exhibit the same gating properties independent of patch configuration (inside-out, outside-out or on-cell), because the tension originating in lipid adherence to glass is the same for each configuration. This description also explains the irreversibility of the conversion, for once lipid anneals to the glass the membrane patch remains under an equilibrium tension. In principle, if it were possible to relieve the tension, we would expect the gating properties to convert back to their initial low-tension values.

Effects of Membrane Tension Induced by Cell Swelling. If the gating conversion induced by gigaseal formation is mediated by increased membrane tension, then similar gating changes should be inducible when a cell membrane is stretched by swelling. To test whether this is the case, K^+ currents were recorded from Sf-9 cells expressing Kv1.2 paddle chimera channels in whole cell mode first under isoosmotic conditions and then sequentially in time following a step to hypoosmotic conditions, which caused the cells to swell over a period of approximately 2.5 min. Osmotic strength was modified using sorbitol to maintain the ionic composition. As cells proceeded to swell the voltage-activation curve shifted to more negative voltages, became slightly steeper, and reached a higher maximum current (Fig. 4 *A* and *C*). These gating changes could be partially reversed upon subsequent transfer to isoosmotic solutions, however, perhaps consistent with incomplete reversibility of gating, cells never returned all the way to their original shape, suggesting that some irreversible mechanical changes to the membrane occur when cells are swollen in this manner (Fig. 4 *D* and *F*). Measurements of electrical capacitance showed the absence of measurable increases in membrane surface area, which we expect should have occurred if channel-containing vesicles were induced to fuse with the membrane during swelling (Fig. 4 *B* and *E*).

The magnitude of the gating conversion was smaller in swollen cells compared to the conversion that occurs upon formation of an isolated gigaseal patch. We suspect that swelling of a cell is less likely to produce the same level of uniform tension increase across the entire cell membrane compared to the uniform increase across an isolated patch. Over the entire cell membrane many of the cytoskeletal attachments remain intact and may interfere with the uniform development of tension. Thus, in the swelling experiment, it is likely that channels in different regions of the membrane experience different levels of lateral tension. A nonuniform population of channels with respect to the degree of conversion would explain why the activation curves are not as steep in the cell swelling experiments, because in this case overall activation is the result of opening channels with different intrinsic midpoints of activation. In conclusion, swelling a cell produces an effect on channel gating that is qualitatively similar to that seen with gigaseal formation. In contrast to lipid adhesion to glass, tension increases caused by cell swelling are at least partially reversible, and thus show that gating conversion appears

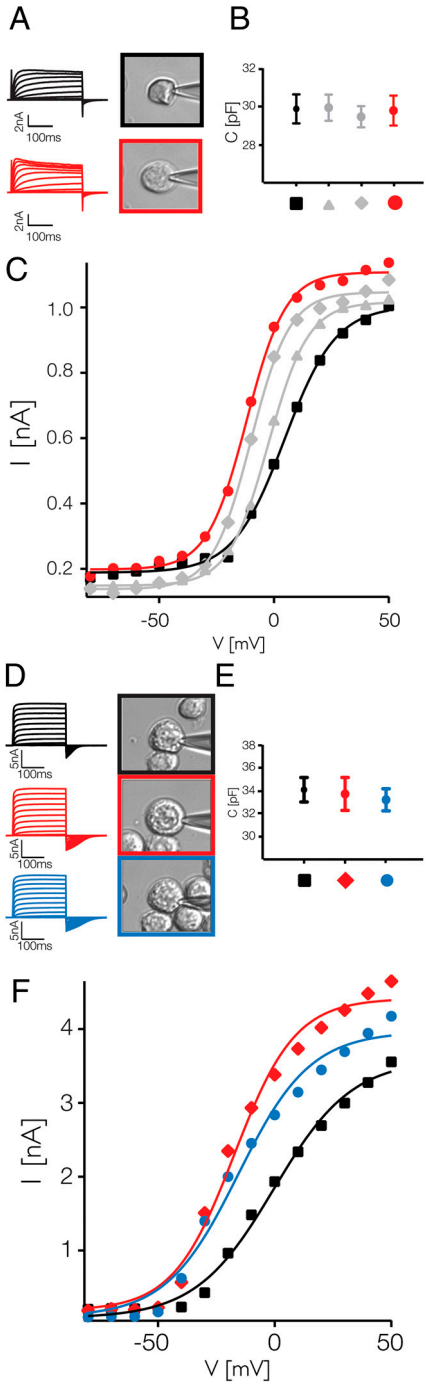

Fig. 4. *The Effect of Swelling by Hypoosmotic Shock. A*, Whole-cell patch recordings of Paddle Chimera expressed in Sf-9 cells during perfusion with isoosmotic (initial volume, black) and hypo-osmotic (peak volume, red). *B*, estimation of the cell capacitance in traces corresponding to initial (black), intermediate (grey) and peak volume (red) state: C (pF): 29.9 ± 0.8, 30.0 ± 0.7, 29.5 ± 0.6, 29.9 ± 0.8. *C*, Boltzmann functions (solid lines) fit data from (A) with V_m (mV) and z (q_e): Black, before swelling: 4.61 ± 0.78, 2.23 ± 0.13. Grey, intermediate swelling states: -2.44 ± 0.26, 2.87 ± 0.08 and -10.05 ± 0.57, 2.96 ± 0.18. Red, peak volume state: -11.95 ± 0.55, 2.92 ± 0.17. *D*, Whole-cell patch recordings of Paddle Chimera expressd in Sf-9 cells during consecutive perfusion with iso-osmotic solution (black), hypoosmotic solution (red), and immediately after peaking volume, iso-osmotic solution (blue). (*E*), estimations of the cell capacitance. C (pF): 34.1 ± 1.1, 33.8 ± 1.4, 33.2 ± 0.9. (*F*), Boltzmann functions (solid lines) fit data from (D) with V_m (mV) and z (q_e): Black, before swelling: -0.35 ± 2.09, 1.49 ± 0.18. Red, during peak volume: -18.56 ± 1.99, 1.67 ± 0.22. Blue, returned to iso-osmotic solution: -17.57 ± 2.63, 1.32 ± 0.2.

to be reversible when membrane tension is returned to a lower value.

A Physical Theory for Tension-Induced Gating Changes in Kv Channels. In Kv channels membrane depolarization drives conformational changes in the four voltage sensors followed by pore opening. This sequence of events is shown in the state diagram,

$$(C_0 \overset{K_1(V)}{\leftrightarrow} C_1 \overset{K_2(V)}{\leftrightarrow} C_2 \overset{K_m(V)}{\leftrightarrow} C_m)^4 \overset{L}{\leftrightarrow} O,$$

in which states C_i inside the bracket represent specific conformations of four voltage sensors undergoing transitions independent of one another and O represents the open pore, achievable once all four voltage sensors have reached their fully depolarized conformation (C_m) (14–16). If, for purposes of reducing the number of parameters, the conformational transitions $K_i(V)$ within each of the voltage sensors are assumed to occur as a single transition (i.e., m = 1 in the state diagram) given by $K(V) = e^{zF(V-V_m)/RT}$ and L is the equilibrium constant for pore opening, then the open probability P_o is given by

$$P_o = \frac{\left[\frac{e^{zF(V-Vm)/RT}}{1+(e^{zF(V-Vm)/RT})}\right]^4 \bullet L}{1 + \left[\frac{e^{zF(V-Vm)/RT}}{1+(e^{zF(V-Vm)/RT})}\right]^4 \bullet L}, \qquad [1]$$

where V is membrane voltage, V_m is the membrane voltage at which a voltage sensor has an 0.5 probability of being depolarized, z the voltage sensor's valence or gating charge, F is the Faraday's constant, and RT is the gas constant times absolute temperature. The current-voltage curves in Fig. 1 have been fit using Eq. **1** with $\langle I \rangle = iNP_o$, where i is the single channel conductance and N the number of channels in the membrane patch. The three curves in each graph, which represent preconversion, intermediate conversion, and postconversion states, can be accounted for by adjusting L alone, the equilibrium constant for pore opening. Variations of K(V) alone do not successfully account for the data (Fig. S2). Moreover, the ability to account for the conversion through variation of L alone does not depend on the assumption that the voltage-dependent transitions within each voltage sensor occur in a single step.

Atomic structures of closed and opened K^+ channels show that pore opening involves a substantial conformational change that expands the pore's cross sectional area within the membrane's inner leaflet (Fig. S3). These conformational differences between closed and opened pore structures offer a possible explanation for how membrane tension could influence the equilibrium constant L. Membrane tension γ will favor an expanded pore by an energy $\gamma\Delta A$, where ΔA is the cross sectional area difference between the closed and opened pore. It follows that L should vary with changes in membrane tension according to

$$\Delta A \Delta \gamma = RT \ln\left(\frac{L_2}{L_1}\right). \qquad [2]$$

In Fig. 1*D* the fits to Eq. **1** give $L_1 = 1.5$ in the low-tension limit and $L_2 = 40$ in the high-tension limit, which, when inserted into Eq. **2**, yield a free energy change of 3.2 RT [2.6 RT for Shaker (Fig. 1*H*), and 5.7 RT for Kv2.1 (Fig. 1*L*)]. The tension change in our experiments is unknown, but if we assume $\gamma = 0$ in the low tension limit and $\gamma = 4$ mN/m = 1 RT/nm^2 as reported by Opsahl and Webb for membrane patches within glass pipettes, then the free energy changes above correspond to an area change ΔA of 3 to 4 nm^2, or approximately a 20% expansion of the pore cross-sectional area. This area change is in the range of what is observed within the inner leaflet for closed and opened K^+ channels in crystal structures. Thus, it seems plausible that increased

membrane tension associated with gigaseal formation could affect the pore-opening transition through this mechanism. What is most interesting is that the energy differences are quite small, in the range of 2.5–6.0 RT units. But through the specific manner in which pore opening is mechanistically connected to voltage sensor movements, these small energy differences result in large changes in the voltage activation curve.

Estimation of the Threshold for Kv Channel Mechanical Activation. To evaluate the tension sensitivity of Kv channel gating we ultimately need to determine the functional relationship between P_o and γ. Unfortunately neither gigaseal formation nor cell swelling allow us to control and know the value of γ. However, using the theory we have developed and assuming that the maximum tension in a gigaseal is 4 mN/m (1 RT/nm^2) we can relate these two quantities through the following thermodynamic equalities. At zero membrane tension we have for the pore opening transition at equilibrium:

$$\Delta G = \Delta G^o + RT \ln L_{\gamma=0} = 0, \quad [3]$$

and at non-zero membrane tension γ:

$$\Delta G = \Delta G^o + RT \ln L_{\gamma} - \gamma \Delta A = 0. \quad [4]$$

Combining Eqs. **2**–**4** yields

$$\gamma = \frac{\ln(\frac{L_\gamma}{L_{\gamma=0}})}{\ln(\frac{L_{\gamma max}}{L_{\gamma=0}})}\gamma_{max}, \quad [5]$$

which relates γ to the maximum tension γ_{max}, taken to be 4 mN/m (1 RT/nm^2), and values of L extractable from the theoretical fits to the voltage activation curves, from which we calculate the open probability P_o.

To assess the consistency of the theory and data, we performed a global fitting analysis on 11 individual patches with Kv1.2 paddle chimera from which 57 families of current-voltage curves were extracted. Each current-voltage curve represents one value of membrane tension γ that was produced either by spontaneous or pressure induced lipid-glass adhesion ranging from the preconversion (low tension) to postconversion (high tension) condition. Each current-voltage data curve was fit using Eq. **1** with $\langle I \rangle = iNP_o$. While the voltage dependence of the voltage-sensor transition, K(V), was constrained to be the same across all patches, the product of channel number and single channel conductance iN was constrained only within the families belonging to the same patch because N varies between patches. Thus, the constraints are consistent with the assumption that gating differences are due solely to membrane tension acting on the pore-opening equilibrium constant L. The results are shown in Fig. S4, Table S1 and Fig. 5.

Fig. 5 relates P_o to γ at different membrane voltages. The first conclusion to be drawn is that the Kv channel is as much a mechanosensitive channel as it is a voltage-dependent channel. At $\gamma = 0$, corresponding to whole cell recordings or patches prior to conversion, P_o as a function of voltage goes from 0 to about 0.65, whereas at $\gamma = 0.5$ RT/nm^2, P_o as a function of voltage goes from 0 to 1.0. As shown explicitly in the graphs in Fig. 5, P_o as a function of γ depends strongly on the value of membrane voltage: mechanosensitivity is diminished at very negative and very positive membrane voltages and is greatest around −20 to −30 mV. For example, a change in membrane tension of 0.4 RT/nm^2 (1.6 mN/m) increases the open probability by 50% at −20 mV, whereas the same change in membrane tension at −50 mV or +20 mV increases it only by 5% or 20%, respectively.

Discussion

Bacterial mechanosensitive channels are high-threshold mechanosensors that evolved to respond at near lytic membrane tensions. These channels were characterized biophysically using the inflation of gigaseal patches. This technique was appropriate for channels such as MscL because at the membrane tensions created by gigaseal formation MscL is closed and it only opens at higher tensions achieved through patch inflation. This high threshold opening makes sense for MscL, given the context under which that channel has evolved to open at very high tensions to prevent cell lysis. In contrast, for three Kv channels tested we observe here a large effect on gating of gigaseal formation without pressurization, which can be attributed to the baseline tension induced by lipid adhesion to glass. Importantly, hypotonic cell swelling also produces similar gating changes. Lipid adhesion to glass produces tension values ranging between 0.5 and 4.0 mN/m (0.125 and 1.0 RT/nm^2). This tension range is considerably lower than that needed to open MscL, and so we call these Kv channels low threshold tension activated channels.

Through quantitative analysis of Kv channel activation curves and a simple theory we show that tension sensitivity of gating can be accounted for if tension acts on the pore opening transition, which follows voltage sensor depolarization. The theory would still work (i.e., would provide an adequate fit to the data) even if we allowed multiple steps in each voltage sensor and permitted L to have some voltage dependence. By including these addi-

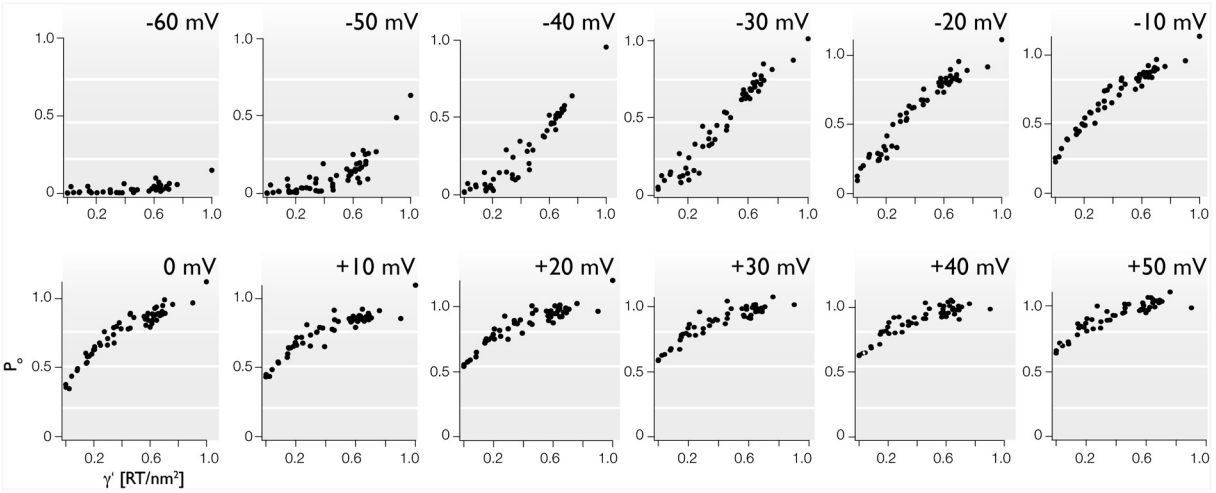

Fig. 5. *Tension Sensitivity at Different Membrane Voltages. A*, Paddle Chimera calculated open probability ($P_o = \langle I \rangle / i^*N$, see Table S1) as a function of calculated membrane tension γ' at different membrane voltages.

tional variables we would diminish the residuals between theory and data (i.e., improve the fit) but the qualitative conclusions would be the same. Moreover, the theory would also work if we assumed that membrane tension could affect L through changes in the pore's shape (i.e., changes in the degree to which the channel matches the membrane's planarity) associated with opening, in addition to its area expansion (17). But the essence of the theory is that membrane tension acts predominantly on the pore opening transition to favor the open conformation, and importantly, the theory does not work if membrane tension acts predominantly on the voltage sensor conformational changes. An important concept to be drawn from this analysis is that tension-induced changes in L corresponding to very small energy differences (i.e., 2.5–6.0 RT units) bring about large changes in the voltage activation curve. In words, this is because the large changes have their origin in the degree to which the voltage sensors act concertedly to open the pore. Large values of L correspond to more concerted coupling between the voltage sensors and the pore.

Finally, it is again instructive to compare the mechanosensitivity of Kv channels to that of MscL. Based on our analysis of membrane tension in numerous patch recordings we deduce that Kv1.2 paddle chimaera's open probability can be raised by 50% at physiological membrane voltages around −20 mV to −30 mV by increasing the membrane tension by 1.6 mN/m (0.4 RT/nm^2). This value is approximately one tenth the tension required to open MscL (3, 4). We envision that this low threshold mechanosensitivity could underlie certain physiological processes in which mechanical forces are converted to electrical signals. For example, opening of Kv channels elicited by mechanical forces to a touch sensitive neuron or muscle contraction could serve to moderate mechanical-induced excitation. Furthermore, because Kv channels are related in structure and function to other voltage-dependent channels including sodium, calcium and nonselective cation channels, we wonder whether they too could exhibit low threshold mechanosensitivity, which could contribute in some circumstances to life's different cellular responses to mechanical forces.

Materials and Methods

Electrophysiology: Patch Clamp Recordings. mRNA encoding the Shaker Kv, Kv2.1 and Paddle Chimera protein subunits was prepared by T7 polymerase transcription and injected into Xenopus laevis oocytes. P3 baculovirus stock coding for Paddle Chimaera subunits was prepared using standard procedures. K^+ currents were recorded in on-cell, inside-out and outside-patches from oocytes five to six days after mRNA injection or in on-cell or whole-cell configuration from Sf-9 cells (Paddle Chimera only) 24–48 h after infection.

For all oocyte patch configurations the extracellular solution contained (mM): 100 KCl, 2 $MgCl_2$, 5 HEPES-KOH pH 7.4 and the intracellular solution contained (mM): 100 KCl, 1 EGTA, 5 HEPES-KOH pH 7.4. Patch pressure was generated using water-filled U-shaped tubing connected to atmospheric pressure and applied via the patch pipette sideport. The pressure was monitored using an in-line manometer (Sper Scientific Ltd.).

For Sf-9 cell patching the extracellular solution contained (mM): 135 NaCl, 10 KCl, 4 $CaCl_2$, 5 $MgCl_2$ and MES-KOH pH 6.4; the intracellular solution contained (mM): 85 KCl, 60 KF, 1 $MgCl_2$, 5 EGTA and 10 HEPES-KOH pH 7.2. For swelling experiments the isoosmotic extracellular solution contained (mM): 100 NaCl, 10 KCl, 4 $CaCl_2$, 5 $MgCl_2$, 10 Glucose and 80 Sorbitol and MES-NaOH pH 6.4. The hypoosmotic extracellular solution lacked Sorbitol. The intracellular solution contained (mM): 85 KCl, 60 KF, 1 $MgCl_2$, 5 EGTA, 10 Glucose and 20 HEPES-KOH pH 7.2. The grounding electrode was separated from the perfused chamber and connected through a salt bridge of low resistance. Perfusion was achieved using a custom-built gravity perfusion system. Cells were patched in whole-cell mode while perfusing with isoosmotic solution. The peak volume change after perfusion of hypo-osmotic solution was seen within 1–3 min, immediately after which cells were returned to isoosmotic solution.

Electrodes were drawn from borosilicate patch glass (VWR) and polished (MF-83, Narishige Co.) to a resistance of 0.8–1.5 M. Analog signals were filtered (1 kHz) using the built-in 4-pole Bessel filter of an Axopatch 200B patch clamp amplifier (Molecular Devices) in patch-mode, digitized at 10 kHz (Digidata 1440A, Molecular Devices) and stored on a computer hard disk.

GUV Formation. Giant Unilamellar vesicles were formed by electroformation. Lipids 1,2-dioleoyl-*sn*-glycero-3-phosphocholine (DOPC, Avanti Polar Lipids) and 1,2-dioleoyl-*sn*-glycero-3-phosphoethanolamine-N-(lissamine rhodamine B sulfonyl) (Rhodamine-DOPE, Avanti Polar Lipids) dissolved in Chloroform at a 200:1 w/w ratio were deposited on clean ITO glass slide (Sigma Aldrich) and dessicated under argon for 1.5 h. The lipids film was rehydrated with 200 mM Sucrose in a custom-built chamber by applying an oscillating DC field using a function generator at the following settings: 120 min, 1 V, 10 Hz; then 50 min, 1 V, 2 Hz. The formed GUVs were diluted into external buffer solution containing 110 mM KCl, 2 mM $MgCl_2$ and used within 24 h.

Data Fitting. Global fitting of G/V datasets was performed using the global fitting package of Igor Pro 6 (Wavemetrics). Each curve is fit to Eq. **1** with $\langle I \rangle = iNP_O$. While the voltage dependence of the voltage-sensor movement, $K(V) = e^{zF(V-V_m)/RT}$, was constrained to be the same across all patches, the product of channel number and single channel conductance (iN) was constrained only within the families belonging to the same patch. For Figs. 2 and 4 and Fig. S1, curves were fitted to the Boltzmann function $I/I\max = 1/1 + e^{(-zF(V-V_m)/RT)}$. The fitting errors are estimated standard deviations of the fitting coefficients.

ACKNOWLEDGMENTS. We thank Jon Sack for providing the Kv2.1 CHO cell line. This work was supported by NIH Grant GM43949. D.S. was supported by the Boehringer Ingelheim Fonds. J.d.M. is a Howard Hughes Medical Institute International Student Fellow. R.M. is an investigator in the Howard Hughes Medical Institute.

1. Sukharev SI, Blount P, Martinac B, Kung C (1997) Mechanosensitive channels of *Escherichia coli*: The MscL gene, protein, and activities. *Annu Rev Physiol* 59:633–657.
2. Hamill O, Martinac B (2001) Molecular basis of mechanotransduction in living cells. *Physiol Rev* 81:685–740.
3. Sukharev S, Sigurdson WJ, Kung C, Sachs F (1999) Energetic and spatial parameters for gating of the bacterial large conductance mechanosensitive channel, MscL. *J Gen Physiol* 113:525–540.
4. Moe P, Blount P (2005) Assessment of potential stimuli for mechano-dependent gating of MscL: Effects of pressure, tension, and lipid headgroups. *Biochemistry* 44:12239–12244.
5. Chang G, Spencer RH, Lee AT, Barclay MT, Rees DC (1998) Structure of the MscL homolog from *Mycobacterium tuberculosis*: A gated mechanosensitive ion channel. *Science* 282:2220–2226.
6. Perozo E, Cortes DM, Sompornpisut P, Kloda A, Martinac B (2002) Open channel structure of MscL and the gating mechanism of mechanosensitive channels. *Nature* 418:942–948.
7. Wiggins PA, Phillips R (2005) Membrane-protein interactions in mechanosensitive channels. *Biophys J* 88:880–902.
8. Ursell T, Huang KC, Peterson E, Phillips R (2007) Cooperative gating and spatial organization of membrane proteins through elastic interactions. *PLoS Comput Biol* 3:e81.
9. Shcherbatko A, Ono F, Mandel G, Brehm P (1999) Voltage-dependent sodium channel function is regulated through membrane mechanics. *Biophys J* 77:1945–1959.
10. Tabarean I, Juranka PF, Morris CE (1999) Membrane stretch affects gating modes of a skeletal muscle sodium channel. *Biophys J* 77:758–774.
11. Opsahl LR, Webb WW (1994) Lipid-glass adhesion in giga-sealed patch-clamped membranes. *Biophys J* 66:75–79.
12. Long SB, Tao X, Campbell EB, Mackinnon R (2007) Atomic structure of a voltage-dependent K^+ channel in a lipid membrane-like environment. *Nature* 450:376–382.
13. Schmidt D, Mackinnon R (2008) Voltage-dependent K^+ channel gating and voltage sensor toxin sensitivity depend on the mechanical state of the lipid membrane. *Proc Natl Acad Sci USA* 105:19276–19281.
14. Hoshi T, Zagotta W, Aldrich RW (1990) Biophysical and molecular mechanisms of Shaker potassium channel inactivation. *Science* 250:533–538.
15. Hoshi T, Zagotta WN, Aldrich RW (1994) Shaker potassium channel gating. I: Transitions near the open state. *J Gen Physiol* 103:249–278.
16. Schoppa NE, Sigworth FJ (1998) Activation of shaker potassium channels. I. Characterization of voltage-dependent transitions. *J Gen Physiol* 111:271–294.
17. Ursell T, et al. (2008) *Mechanosensitivity in Cells and Tissues 1: Mechanosensitive Ion Channels* (Springer, Berlin).